ACCV2002: The 5th Asian Conference on Computer Vision, 23-25 January 2002, Melbourne, Australia.

A method for noise removal and object detection based on data expansion by multiresolution representation and data compression by principal component analysis

Jean-Baptiste Fasquel, Christophe Stolz and Michel Bruynooghe
Photonics Systems Laboratory, Louis Pasteur University
Bld Sebastien Brant, 67400 Illkirch, France
fasquel@apia.u-strasbg.fr

Abstract

This paper presents a method for noisy object detection which is based on the expansion/compression paradigm and combines a multiresolution approach with the principal component analysis (PCA). The multiresolution representation is done by successive Gaussian filterings. The compression of the expanded information is achieved by only keeping the first PCA factorial image. Endly, the object of interest is detected and delineated from the previous factorial image by using a standard valley thresholding technique. The proposed method behaves as a compromise between the various Gaussian filterings by limiting the blurring effect of such filterings and removing most of the noise. The experimental evaluation using synthetic objects has shown the ability of this approach to clean strongly noisy images. For scenes containing several objects of interest, like CT-Scan images, we first search for regions of interest (ROIs). Then, for each ROI, we locally apply the proposed detection method. Experimental results have shown the potential of the proposed method for the detection of liver tumours from CT-Scan images and for the segmentation of handwritten characters.

1. Introduction

The detection of noisy objects is a classical problem encountered in most vision systems. To solve this problem, many approaches and techniques have been developped. A classical approach is the region based approach. The goal of methods based on such an approach is to smooth the different regions without removing the boundaries between them. Image smoothing can be performed using either isotropic diffusion or anisotropic diffusion. The current limitation of isotropic diffusion is the blurring effect of edges and the uncorrect noise removal when no knowledge about the noise is available [6]. To avoid these limitations, Perona and Malik [8] have proposed the anisotropic diffusion which consists in smoothing the regions without blurring their edges. But the quality of this smoothing strongly depends on the number of iterations, which may lead to a really time consuming processing [5]. Moreover, this approach requires a supervised definition of several parameters. To overcome these drawbacks, we propose an unsupervised method based on the expansion/compression paradigm [7] which combines a multiresolution approach [1] and the principal component analysis (PCA) [9]. The multiresolution representation is achieved by successive Gaussian filterings. The compression of the expanded information is carried out using PCA. Then, the denoised image is the so called first factorial image obtained by keeping the highest eigenvalue only. This unsupervised method aims to find the best compromise between a too strong blurring and a too weak noise removal.

In the following section, we describe the detection method. In the third section, we study the behaviour of the proposed method with respect to the degree of noise and the object size. In the fourth section, we illustrate the potential of the proposed method for liver tumour detection and segmentation of handwritten characters. Finally, we conclude on this unsupervised detection method.

2. Method

The proposed detection method is based on the expansion/compression paradigm (E/C)[7]. This is a general approach for extracting features for pattern recognition applications. Essentially, this E/C paradigm first expands the input signal in some transform domain and then compresses the resulting expansion for presenting to a classifier. In our case, the transformation is the Gaussian transform and consists in applying a succession of Gaussian filterings of in-

creasing width to the original noisy image $f(x,y)$. Each Gaussian filtering, characterized by the width of the Gaussian filter σ_i, leads to a transformed image $f_i(x,y)$:

$$f_i(x,y) = \int\int f(a,b) exp[-(\frac{(a-x)^2+(b-y)^2}{2\sigma_i^2}] \, dadb. \quad (1)$$

Such Gaussian filterings lead to the multiresolution representation [1, 2] of the original noisy image $f(x,y)$. As usually considered in multiresolution analysis, we operate an octave decomposition by choosing $\sigma_i = 2^i$, with $i = [0, 1, ..., n]$. Then, the compression enables to reduce the redundancy of the representation and consists in the principal component analysis (PCA). To perform such a compression, we consider each Gaussian filtered image $f_i(x,y)$ as a column vector $\overrightarrow{x_i}$ whose length k is equal to the number of pixels of the analyzed image. Then, the PCA is applied to the matrix X whose columns are the n image vectors $\overrightarrow{x_i}$:

$$X = [\overrightarrow{x_1}, ..., \overrightarrow{x_n}]. \quad (2)$$

The PCA decomposes the information contained in image data by creating a series of so-called factorial images $F_1, F_2, ...$ of decreasing variance. To begin this transformation, image vectors $\overrightarrow{x_i}$ are centered by substraction of their mean μ_i, and normalized by their standard deviation s_i. This leads to the data matrix A:

$$A = [\overrightarrow{t_1}, ..., \overrightarrow{t_n}]. \quad (3)$$

Then, the correlation matrix, C, is computed:

$$C = \frac{1}{k} A^T A, \quad (4)$$

where the superscript T represents the matrix transpose operator.

The PCA states that there is an orthogonal matrix $V = [\overrightarrow{v_1}, ..., \overrightarrow{v_n}]$ and a diagonal matrix D such that $A^T A = VDV^T$. The columns of V are the eigenvectors of $A^T A$ and form an orthonormal basis. The diagonal entries of D are the eigenvalues λ_i of $A^T A$ and are sorted by decreasing order so that $\lambda_j \geq \lambda_{j+1}$ for $j = 1, ..., n$.

The first p factorial images F_i, with $i = 1, 2, ..., p$, which correspond to eigenvalues λ_i, are computed by projection of centered and normalized image data on the eigenvectors $\overrightarrow{v_1}, ..., \overrightarrow{v_p}$:

$$\overrightarrow{F_i} = A \times \overrightarrow{v_i}. \quad (5)$$

$\overrightarrow{F_i}$ denotes the factorial image vector related to the factorial image F_i. These linear projections lead to p uncorrelated factorial images. The choice of the number p of factorial images will based on a visual perception criteria as explained hereafter.

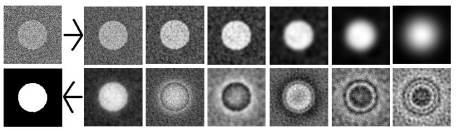

Figure 1: Application of the proposed method for the detection of a noisy disc of diameter of 128 pixels. **First line:** Initial noisy model and the corresponding set of six Gaussian filterings. **Second line:** The set of factorial images, sorted by decreasing order of their eigenvalues and the thresholded first factorial image (binary disc on the left side). We see that the first factorial image contains most of the significant information.

The figure 1 gives the example of a noisy disc detected by the proposed method. The first line represents the initial noisy disc and the set of six Gaussian filterings used for the expansion. The second line represents the set of factorial images, sorted by decreasing order of their eigenvalues, and the thresholded first factorial image (left side). The visual observation of the first factorial image clearly shows that most of the noise has been removed without blurring the object boundary. Furthermore, this factorial image explains about 90% of the total variance of the set of centered and normalized Gaussian filtered images. The following factorial images ($F_2, F_3, ...$) are more noisy and do not contain useful additional information from the point of view of visual perception. Consequently, it is enough to only consider the first factorial image F_1.

Finally the object is detected and delineated using the standard valley thresholding technique which is applied to the first factorial image F_1. This thresholding is illustrated by the binary object on the left side of the second line of the figure 1. This shows that the noisy disc has been correctly delineated. This furthermore justifies the choice of only keeping the first factorial image.

The first factorial image is a linear combination of the six Gaussian filterings which can be interpreted as a compromise between a too weak smoothing which would not remove enough noise and a too strong filtering which would blur the object boundaries.

3. Evaluation of the object detection method

We propose to study the behaviour of the proposed method with respect to the type and degree of noise corrupting the images and to the object size. For this analysis, we consider a given set of Gaussian filters defined by $\sigma_i = [1, 2, 4, 8, 16, 32]$.

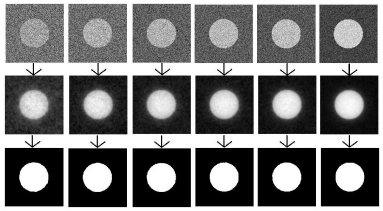

Figure 2: **First line:** set of discs of diameter 32 pixels corrupted by increasing additive gaussian noises characterized by the resulting $SNRs = [0.00, 7.04, 12.04, 15.91, 19.08, 27.95]$, in dB. **Second line:** the resulting set of factorial images.**Third line:** the set of thresholded factorial images.

3.1. Influence of Gaussian additive noise

We assume that the signal $f(x, y)$ we want to denoise is an ideal signal corrupted by an additive noise. We propose to represent the noise as a normally distributed (Gaussian), zero-mean random process with a probability density function $f_x(x)$ [3]:

$$f_x(x) = \frac{1}{\sqrt{2\pi}\sigma} e^{-\frac{x^2}{2\sigma^2}} \tag{6}$$

where σ is the noise standard deviation. The effect of an additive noise process, n, on the image $f(x, y)$ can be defined as the summation of the true signal $s(x, y)$ with the noise:

$$f(x, y) = s(x, y) + n(x, y). \tag{7}$$

For this study, we considered that the ideal signal is a disc a diameter 32 pixels corrupted by various additive Gaussian noises leading to signal to noise ratios (SNRs) of $[0, 7.04, 12.01, 15.91, 19.08, 27.9]$ in dB. The first line of figure 2 shows the set of noisy discs corresponding to the various SNRs. The second line (resp. third line) shows the resulting factorial images (resp. the resulting delineated discs). We see that the initially noisy discs are correctly delineated.

The factorial image is a linear combination of the six Gaussian filterings whose weights are the coordinates of the first eigenvector. More precisely, in our case: the first coordinate gives the weight of the first Gaussian filtering defined by a width of 1 pixel, the second coordinate gives the weight of the second Gaussian filtering defined by a width of 2 pixels, and so on, up to the strongest Gaussian filtering defined by a width of 32 pixels. The figure 3 shows that Gaussian filtering weights depend on SNRs. In particular, when the noise increases, the influence of the weak Gaussian filterings decreases. This shows that the PCA compression takes automatically into account the degree of noise corrupting the image without any a priori knowledge about it.

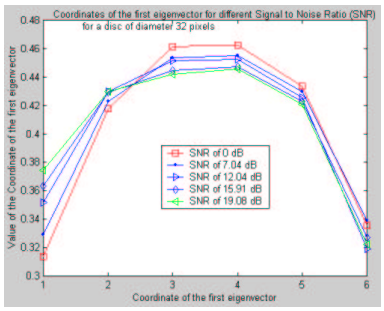

Figure 3: Values of the six coordinates of the first PCA eigenvector for different SNRs, in the case of a disc of diameter 32 pixels. This shows the evolution, with respect to the SNR, of these coordinates which are the weights involved in the linear combination of the six Gaussian filterings leading to the factorial image.

3.2. Influence of Gaussian multiplicative noise

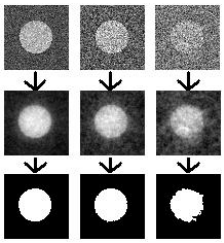

Figure 4: Three discs of diameter 32 pixels, corrupted by multiplicative Gaussian noises, characterized by $\sigma = [0.025, 0.05, 0.1]$. The relative contrast of the model is of 0.05. **First line:** the three noisy discs. **Second line:** the corresponding three factorial images. **Third line:** the resulting thresholded factorial images.

Many acquisition systems lead to data corrupted by a multiplicative noise. For this reason, we propose to evaluate the ability of the proposed method to remove such kind of noise. The multiplicative noise can be defined by a unitary-mean normal random process with a probability density function of [3]:

$$f_x(x) = \frac{1}{\sqrt{2\pi}\sigma} e^{-\frac{(x-1)^2}{2\sigma^2}} \tag{8}$$

where σ is the standard deviation of the noise process. The effect of such a multiplicative noise process, m, on the image $f(x, y)$ can be defined as being the multiplication of the true signal $s(x, y)$ with the noise:

$$f(x, y) = m(x, y).s(x, y). \tag{9}$$

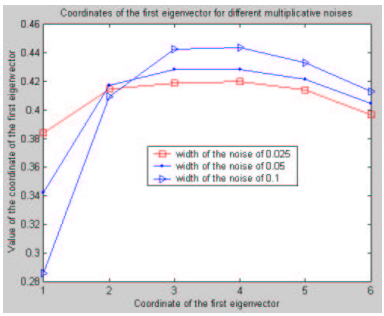

Figure 5: Case of a disc of diameter of 32 pixels corrupted by various multiplicative gaussian noises: coordinates of the first PCA eigenvector corresponding to the weights defining the linear combination of the six Gaussian filterings. The behaviour of these weights is similar to the behaviour observed in the case of an additive Gaussian noise.

For the tests, image grey levels are supposed to vary between 0 and 1. We considered an ideal disc of diameter 32 pixels, with a relative contrast of 0.05. More precisely, the grey level of the disc (resp. background) is 0.525 (resp. 0.475). This ideal disc is then corrupted by three different multiplicative Gaussian noises characterized by the following relative standard deviations: $\sigma = [0.025, 0.05, 0.1]$. The figure 4 shows the three noisy discs (first line), the corresponding factorial images (second line) and their resulting thresholdings (third line). We see that, in each case, the object of interest has been correctly detected and delineated, as shown by visual comparison with the initially noisy version. The figure 5 gives the distribution of the coordinates of the first eigenvector. The evolution of these weights is similar to the evolution observed in the case of an additive Gaussian noise. For this reason, in the following tests, we will only consider objects corrupted by an additive gaussian noise.

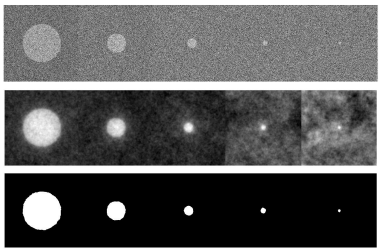

Figure 6: Set of disc of varying sizes, initially corrupted by an additive Gaussian noise corresponding to a SNR of 0 dB. **First line:** the set of initially noisy discs. **Second line:** the set of factorial images. **Third line:** the set of resulting thresholdings. The discs are correctly detected.

3.3. Influence of object size

We applied the proposed method to noisy discs of varying diameters d being, in pixels: $d = [10, 16, 32, 64, 128]$. Each disc was initially corrupted by a Gaussian additive noise corresponding to a SNR of 0 dB. The figure 6 shows the different initially noisy discs (first line), the factorial images (second line) and the resulting thresholdings (third line) obtained for the different sizes. We see that, in each case, the noisy disc has been correctly detected.

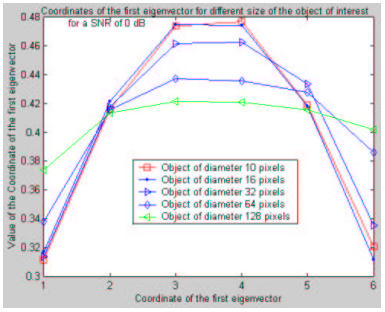

Figure 7: Coordinates of the first PCA eigenvector for different object sizes. The SNR is fixed to 0 dB.

The figure 7 gives the distribution of the weights characterizing the PCA compression with respect to the various object sizes. It can be observed that this weight distribution depends on the object size: when the size of the disc decreases, the weights corresponding to both weakest and strongest filtering decreases. This shows that the PCA analysis selects automatically the weights so that small objects do not disappear because of a too strong smoothing.

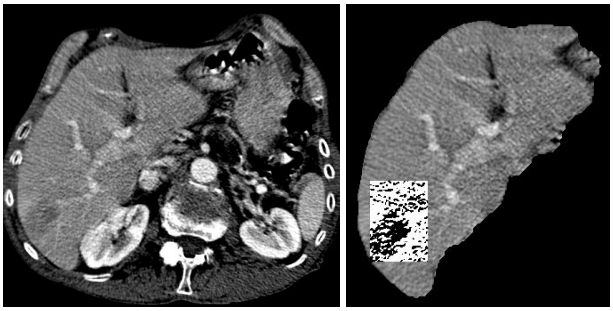

Figure 8: Example of tumour in the liver. **Left side:** example of slice of abdomen. **Right side:** Segmented Liver. The highlighted and thresholded area contains a tumour. This tumour appears as a dark and compact object which is difficult to automatically detect and correctly delineate.

4. Illustration of the potential of the proposed method

The potential of the proposed method is illustrated by processing some images encountered in two different applications: the detection of liver tumours from CT-Scan images and the segmentation of handwritten characters.

4.1. Liver tumour detection from CT-Scan images

The main purpose of the computer aided diagnostic of the liver is to segment automatically the liver and the different structures such as vessels and tumours from a set of about hundred slices acquired by a CT-Scanner [10]. Each slice is an image of 512x512 pixels. The pixel size is $0.65 \times 0.65mm^2$.

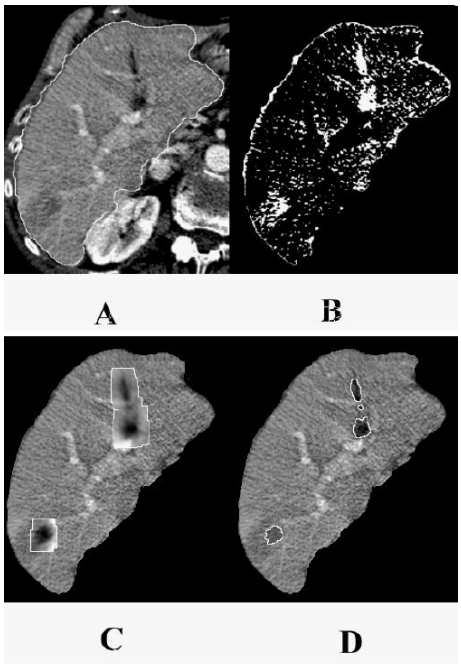

Figure 9: Illustration of the different steps: **A:** a liver slice. **B:** its thresholded version showing the existence of granular noise. **C:** incrustation of the factorial images of the two ROIs within the original image. **D:** The four delineated objects: the tumour to be detected (bottom, left) and three false alarms corresponding to normal anatomical structures (top, right-center).

Our detection method will be applied to the segmentation and delineation of liver tumours, appearing darker than the parenchyma as shown on the figure 8-Left. The figure 8-Right corresponds to the segmented liver within which a region of interest containing the tumour has been thresholded. The granular aspect of this thresholded image shows the difficulty of the tumour delineation. This justifies the need of a smoothing process. Tumours are of varying sizes and of varying contrasts [10]. We first search for regions of interest (ROIs) containing tumours of various sizes. For this purpose, we initially threshold the original image, perform a morphological alternate sequential filtering to remove the granular noise, and then close the binary filtered image using a larger structuring element. The ROIs are obtained by searching for the connected components of the closed thresholded image. Finally, for each ROI, we locally apply our detection method. Additional details are given in our previously published work dealing with the opto-electronic implementation of the proposed method for tumour detection [4]. The figure 9 illustrates the different steps leading

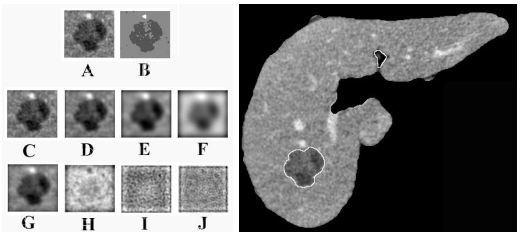

Figure 10: Illustration of the details of the processing for detecting a liver tumour using four Gaussian filterings defined by $\sigma = [2, 4, 8, 16]$: **A:** the initial tumour. **B:** thresholded initial tumour **C, D, E, F:** the four Gaussian filterings of the initial tumour in increasing order of the width of the related Gaussian filters. **G, H, I, J:** the four factorial images, sorted by decreasing order of their eigenvalues. G is the first factorial image which corresponds to the highest eigenvalue and contains the significant visual information. The other factorial images are mostly noisy. The liver slice on the right side shows the resulting contour of the delineated tumour obtained by thresholding the first factorial image G.

to the detected tumour and to three false alarms. The figure 10 shows the details of the processing of the ROI containing the tumour belonging to the slice displayed on the right side. Our detection method has been applied to fifteen liver slices, using four Gaussian filterings defined by $\sigma = [2, 4, 8, 16]$ [4]. The results have been analyzed by the medical staff of our medical partner IRCAD (Institut de Recherche sur le Cancer de l'Appareil Digestif). Several conclusions can be extracted from this analysis [4]. First, most tumours are correctly depicted. Secondly, the segmentation precision has been visually validated as correct.

4.2. Handwritten character segmentation

Currently, there is a substantial and growing interest in the field of document image processing and understanding

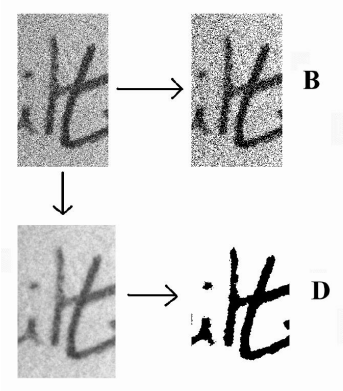

Figure 11: **A:** a noisy character. **B:** its thresholded version showing the existence of granular noise and the difficulty of the segmentation task. **C:** the factorial image. **D:** the thresholded version of C. The initially noisy handwritten character is correctly segmented.

[2]. Document analysis consists in first extracting writtings, and then classifying them. Here, we illustrate the potential of our detected method for the segmentation of handwritten characters from noisy gray-level images. We assume that the objects (characters) have a relatively constant size (width of the strokes). Hence, we do not have the problem encountered in the previous medical application where objects were of various sizes. To carry out the feasability test, handwritten characters have been digitized, using an AGFA scanner at 400 dpi resolution. On the resulting digitized image, the width of the strokes was of about 15 pixels. For the feasability test, we used four Gaussian filterings characterized by $\sigma = [2, 4, 8, 16]$. The figure 11 shows an example of a character segmented by our method. After the thresholding of the first factorial image (figure 11-C), the character is correctly delineated (figure 11-D). Such a preliminary experimental result illustrates the potential of the proposed method for this application.

5. Conclusion

This paper proposes an unsupervised method for the detection of noisy objects which is based on the expansion/compression paradigm, using the multiresolution representation with various Gaussian filterings and the principal component analysis (PCA). This unsupervised method automatically leads to an acceptable compromise between various Gaussian filterings. The efficiency of this approach has been evaluated with respect to the degree of noise and to the object size. The experimental analysis has shown the ability of this approach to clean noisy images corrupted with additive or multiplicative gaussian noise.

Two practical applications have been considered to illustrate the potential of the proposed method. These applications dealt with the liver tumour detection and the segmentation of handwritten characters. Preliminary experimental results are promising. Nevertheless, further experiments must be carried out to validate the efficiency of the proposed method on large databases.

References

[1] K. R. Castleman. *Digital Image Processing*. Prentice Hall, 1996.

[2] M. Cheriet. Extraction of handwritten data from noisy gray-level images using a multiscale approach. *International Jounal of Pattern Recognition and Artificial Intelligence*, 13(5):665–684, 1999.

[3] B. R. Corner, R. M. Narayanan, and S. E. Reichenbach. Principal component analysis of remote sensing imagery: effects of additive and multiplicative noise. In *Proc. SPIE on Applications of Digital Image Processing XXII*, volume 3808, pages 183–191, 1999.

[4] J. B. Fasquel, M. Bruynoogh, and P. Meyrueis. A hybrid opto-electronic processor for the delineation of tumours of the liver from ct-scan images. *SPIE The International Symposium on Optical Science and Technology, San Diego, USA*, Wave Optics for Optical Information Processing, July 2001.

[5] B. Fischl and E. L. Schwartz. Adaptive nonlocal filtering: A fast alternative to anisotropic diffusion for image enhancement. *IEEE Transactions on Pattern Analysis and Machine Intelligence*, 21(1):42–48, 1999. January.

[6] R. Gonzales and P. Wintz. *Digital Image Processing, 2nd edition reading*. Addison-Wesley, 1987.

[7] G. Okimoto and D. Lemonds. Principal component analysis in the wavelet domain: New features for underwater object recognition. In *Proc. SPIE on Detection and Remediation Technologies for Mines and Minelike Targets IV*, volume 3710, pages 697–708, 1999.

[8] P. Perona and J. Malik. Scale-space and edge detection using anisotropic diffusion. *IEEE Transactions on Pattern Analysis and Machine Intelligence*, 12(7):629–639, July 1990.

[9] R. J. Schalkoff. *Pattern Recognition: statistical, structural and neural approaches*. John Wiley, Inc, 1992.

[10] L. Soler, H. Delingette, G. Malandain, J. Montagnat, N. Ayache, C. Koehl, O. Dourthe, B. Malassagne, M. Smith, D. Mutter, and J. Marescaux. Fully automatic anatomical, pathological, and functional segmentation from ct scans for hepatic surgery. *Computer Aided Surgery*, 6(3), August 2001.